



HAL
open science

A generalization of CAPE into potential energy convertibility

Jun-Ichi Yano, Jean-Pierre Chaboureau, Françoise Guichard

► **To cite this version:**

Jun-Ichi Yano, Jean-Pierre Chaboureau, Françoise Guichard. A generalization of CAPE into potential energy convertibility. *Quarterly Journal of the Royal Meteorological Society*, 2005, 131 (607), pp.861-876. <10.1256/qj.03.188>. <hal-00068827>

HAL Id: hal-00068827

<https://hal.science/hal-00068827v1>

Submitted on 12 Aug 2021

HAL is a multi-disciplinary open access archive for the deposit and dissemination of scientific research documents, whether they are published or not. The documents may come from teaching and research institutions in France or abroad, or from public or private research centers.

L'archive ouverte pluridisciplinaire HAL, est destinée au dépôt et à la diffusion de documents scientifiques de niveau recherche, publiés ou non, émanant des établissements d'enseignement et de recherche français ou étrangers, des laboratoires publics ou privés.



Distributed under a Creative Commons CC BY 4.0 - Attribution - International License

A generalization of CAPE into potential-energy convertibility

By JUN-ICHI YANO^{1*}, JEAN-PIERRE CHABOUREAU² and FRANÇOISE GUICHARD¹

¹*CNRM-GAME (CNRS and Météo-France), France*

²*Laboratoire d'Aerologie, Observatoire Midi-Pyrenees, France*

The concept of the potential-energy convertibility (PEC) is proposed as a generalization of convective available potential energy (CAPE). It is defined as a vertical integral of buoyancy weighted by a non-dimensional normalized vertical momentum. This is a measure of convertibility of potential energy into kinetic energy in the sense that the actual conversion rate is recovered when PEC evaluated by the convective-scale local buoyancy and vertical momentum, as available from cloud-resolving model (CRM) simulations, is multiplied by the normalization factor for the vertical momentum. It reduces to CAPE, when the standard parcel-lifted buoyancy and a unit value for the normalized vertical momentum are used. It is equivalent to Arakawa–Schubert’s cloud work function, when the buoyancy and the vertical momentum profile for an entraining plume are used. PEC evaluated from locally defined buoyancy and vertical momentum in CRM simulations correlates better with the convective precipitation than CAPE. The evaluation of PEC within a convective parametrization may be possible with an appropriate definition of the effective entrainment rate, for example, which is expected to improve CAPE-based convective parametrizations.

KEYWORDS: Convective parametrization Energy cycle PEC

1. INTRODUCTION

The convective available potential energy (CAPE), originally introduced by Moncrieff and Miller (1976), is a commonly used quantity as a measure of moist-convective instability (conditional instability) of the atmosphere (cf. Roff and Yano 2002; see also Emanuel 1994). However, in spite of its name, CAPE cannot be directly identified as a part of standard energy cycles in the atmospheric dynamics. In the standard description of the global atmospheric dynamics (e.g. Holton 1992, section 10.4), the energy cycle is defined by the exchange between the kinetic energy and the available potential energy, with the latter defined as a ‘convertible’ part of the *total* potential energy. This energy cycle is naturally derived by applying the standard procedure of the energy integral (cf. Goldstein *et al.* 2002) to the primitive-equation system, or to the non-hydrostatic anelastic system.

As far as such a formal energy cycle is concerned, the inclusion of convective heating effects does not change its formulational structure, into that CAPE does not enter. The latter is defined by a heuristic process associated with a hypothetical pseudo-adiabatic lifting of an air parcel, independent of this formal description.

In the present paper, we are going to argue that CAPE is better interpreted as a measure of *convertibility* of the potential energy into the kinetic energy, rather than as a potential energy. This point is, in fact, already stated mathematically by Eq. (132) of Arakawa and Schubert (1974), but without further physical remarks, in introducing the cloud work function, which is typically interpreted as a natural extension of CAPE to entraining plumes (cf. Mapes 1997; Brown and Zhang 1997; Yano 1999; Donner and Phillips 2003). Here, the standard CAPE is defined for a hypothetical lifting of an air parcel without mixing (i.e. undiluted).

We will develop our argument by stepwise physical considerations in the next section. This naturally leads to a further generalization of the concept of CAPE. We call

* Corresponding author: CNRM-GAME, Météo-France, 42 av Coriolis, 31057 Toulouse Cedex, France.
e-mail: yano@cnrm.meteo.fr.

it the potential-energy convertibility (PEC), in which a general profile of vertical velocity is considered in place of that for an entraining plume as in the cloud work function, or a constant uplifting as in the original CAPE. This quantity provides a *normalized* rate of generation of the kinetic energy from the available potential energy, when a local vertical velocity is used along with actual buoyancy felt by the local air mass instead of that for a hypothetically lifted air parcel.

As shown by Sherwood (1999), CAPE does not work as a statistically useful predictor of deep convection in the tropical atmosphere. A substantial amount of CAPE *almost* always exists in the tropical atmosphere (cf. Roff and Yano 2002, Fig. 1), but deep convection is triggered only intermittently. In this respect, CAPE is not a good measure of moist-convective instability either. This becomes more practical problems (e.g. Guichard *et al.* 2004) when such a hypothetical lifting process of an air parcel, as for computing CAPE, is used in convective parametrizations for determining both the existence and the degree of convection (e.g. Fritsch and Chappell 1980; Kain and Fritsch 1990; Zhang and McFarlane 1995; Gregory *et al.* 2000; Bechtold *et al.* 2001). A generalization of CAPE is expected to be useful for this reason, too. A type of generalization has already been proposed by Randall and Wang (1992) with a name of the Generalized CAPE. Here, we propose an alternative possibility.

In section 3, we show that PEC works as a better measure of moist-convective instabilities than the standard undiluted definition of CAPE, by applying this concept to four examples of cloud-resolving model (CRM) simulations. Some of the parametrizations are currently shifting to a CAPE definition based on an entraining parcel (e.g. Jakob and Siebesma 2003; Kain 2004). The present work is expected to contribute positively to this current effort by providing a potential methodology for objectively evaluating an *effective* entrainment rate based on the PEC computations from CRM. These possible applications of PEC are discussed in the concluding section.

2. THEORY

Imagine that an air parcel of a unit mass (say 1 kg) is lifted from a surface layer. In this hypothetical lifting process, the air parcel does not mix with the surrounding environmental air, but maintains the same pressure with the environment at every step of lifting. Such a lifting process is totally hypothetical, but a standard procedure for considering convective instabilities in meteorology (e.g. Rogers and Yau 1989).

Normally, the atmosphere is stably stratified in such sense that an air parcel feels a negative buoyancy (i.e. $b < 0$ with b N kg⁻¹ the buoyancy) by its vertical lifting over a short distance. However, a different situation may arise when the air parcel is lifted further upwards. The lifted air parcel becomes saturated at a certain vertical level (i.e. lifting condensation level), and a further lifting leads to a warming of the parcel by latent heating associated with condensation of saturated water vapour.

This condensational heating may overcompensate the adiabatic cooling associated with the lifting. As a result, the lifted parcel may become warmer than the environment (hence positive buoyancy $b > 0$ results) above a certain vertical level (i.e. level of free convection), hence this hypothetical air parcel may be destabilized by an uplifting of a finite distance. This is traditionally considered as a basic mechanism for moist-convective instability, which is also called *conditional instability*, being conditioned by a lifting of the air parcel over a finite critical distance.

Note that, under this hypothetical lifting process, the parcel buoyancy b is defined by the difference of virtual temperatures for the air parcel and the environment, with the latter typically measured by a synoptic-scale state as either directly measured by

soundings or defined as a grid-column profile within a global model. The surface layer values of these synoptic-scale mean states are typically used for this hypothetical lifting of the air parcel.

The resulting positive buoyancy b performs work

$$dW = b dz \quad (1)$$

on this air parcel by an infinitesimal lifting over dz . When the air parcel is lifted from a level z_1 to z_2 , the work performed by buoyancy is given by an integral over this vertical range, i.e.

$$W = \int_{z_1}^{z_2} b dz, \quad (2)$$

which may be converted into the kinetic energy. This constitutes the definition of CAPE, in which z_1 is normally taken either at the surface or at the level of free convection, z_2 at the highest level that neutral buoyancy is attained (i.e. the level of neutral buoyancy). The vertical integral in Eq. (2) may also be limited to the zones where buoyancy is positive.

From this argument, it transpires that CAPE is more directly defined as *work* rather than as potential energy. Here, thermodynamically, work constitutes a process that converts potential energy into kinetic energy (see, e.g. ter Haar and Wergeland (1966) for more concrete discussions). Such hypothetical work constitutes potential energy only if the force is defined by a potential (cf. Goldstein *et al.* 2002). The buoyancy is not defined by a potential, so the work defined by Eq. (2) does not constitute potential energy in the sense of classic mechanics.

A few difficulties in defining CAPE may be pointed out from this perspective. Most obviously, the estimate of buoyancy is based on a hypothetical lifting process of an *undiluted* air parcel. In some convective parametrizations (cf. Jakob and Siebesma 2003; Kain 2004), this limitation is amended in the closure by mixing the lifting air parcel with environmental air with a certain rate (i.e. entrainment rate). On the other hand, in cloud-resolving model experiments, this definition can be more directly replaced by the actual buoyancy felt by the local air, as defined under the anelastic formulation (cf. Lipps and Hemler 1982; Durran 1989), as will be done in the following analyses. This latter point also motivates the following generalization.

The above definition does not say anything about the time-scale of this energy conversion process, either. The faster the lifting process, the more energy is generated in a given time with the same CAPE. As a related aspect, the definition of CAPE just described is based on a Lagrangian picture, which measures an energy conversion process along a parcel trajectory. Such a Lagrangian description is not quite compatible with our standard Eulerian descriptions of the system in numerical modellings.

This very last aspect is most easily taken into account by reformulating the description. We simply need to apply a time derivative on Eq. (1), which leads to:

$$\frac{dW}{dt} = b \frac{dz}{dt} = bw. \quad (3)$$

Here, the vertical velocity w is introduced by $w \equiv dz/dt$. A vertical integral of Eq. (3) provides a rate of generation of kinetic energy for a given atmospheric column:

$$\int_0^H \rho \frac{dW}{dt} dz = \int_0^H \rho w b dz. \quad (4)$$

Here, the density ρ is multiplied on the integrand so that the energy generation rate per column (i.e. $W \text{ m}^{-2}$) is obtained after integration. We have set $z_1 = 0$, defined

as the surface, and $z_2 = H$, the tropopause height, so that the integral over the whole troposphere is performed.

By comparing Eq. (4) with Eq. (2), we see that CAPE can be interpreted as a rate of generation of kinetic energy by a hypothetical lifting of air parcel with a unit vertical momentum, $\rho w = 1$. By multiplying this hidden unit factor 1 ($\text{kg m}^{-3} \text{m s}^{-1}$) on CAPE (J kg^{-1}), it also embodies a unit of energy conversion rate. In this manner, more precisely, CAPE is interpreted as a measure of the capacity of buoyancy to generate kinetic energy by consuming the potential energy. The actual energy conversion rate is also proportional to the degree of vertical motions, hence it is estimated by multiplying a measure of vertical momentum (*or* mass flux), say, $(\rho w)^*$ on CAPE. This interpretation also provides a translation of CAPE as originally defined under a Lagrangian framework into an Eulerian framework.

Conversely, we can generalize the concept of CAPE as a rate of conversion of energy (Eq. (4)) normalized by a measure of the vertical momentum $(\rho w)^*$, i.e.

$$\text{PEC} \equiv \int_0^H \rho w b \, dz / (\rho w)^*, \quad (5)$$

and call it the potential-energy convertibility (PEC). Here, as a normalization factor $(\rho w)^*$, we take a root mean square of the vertical momentum over the atmospheric column, i.e.

$$(\rho w)^* \equiv \left\{ \overline{\int_0^H (\rho w)^2 \, dz / H} \right\}^{1/2} \quad (6)$$

in the following. The horizontal-domain mean is applied on $(\rho w)^*$, as designated by the overbar, in order to facilitate a separation of the generation rate of kinetic energy into contributions from the buoyancy forcing (i.e. PEC) and from the vertical motions (i.e. $(\rho w)^*$) in terms of the domain-mean budget, as in the following analyses. Thus, the rate $(\rho w)^* \text{PEC}$ of conversion of available potential energy into the kinetic energy is defined by the two factors: the degree of the vertical motion, measured by $(\rho w)^*$, and the degree of buoyancy forcing, measured by PEC, in the domain-mean energy budget.

It can be easily verified, more directly from the standard energy integral (see e.g. Chandrasekhar 1961; Holton 1992), that $(\rho w)^* \text{PEC}$ provides the actual conversion rate from the potential energy to the kinetic energy, when locally defined buoyancy b and vertical velocity w are used as given in CRM simulations (cf. Xu *et al.* 1992, Eqs. (7)–(9)). By defining PEC in this manner, we are going to show in the next section that it provides a better measure of moist-convective instabilities of the system in CRM experiments.

As a standard definition of PEC, we propose to use both the buoyancy b and the vertical velocity w as locally measured in a convective system, as readily available from a CRM experiment. The results of the next section are based on this definition. Various different choices are possible for both b and the normalized vertical momentum $\rho w / (\rho w)^*$. Most importantly, PEC reduces to CAPE by taking the unit vertical momentum $\rho w / (\rho w)^* = 1$. The standard CAPE adopts the undiluted parcel buoyancy for b , but the lifting-parcel buoyancy can also be computed assuming a finite mixing with an environment as done for the revised Kain–Fritsch scheme (Kain 2004), for example. Arakawa and Schubert’s (1974) cloud work function assumes an entraining plume both for b and $\rho w / (\rho w)^*$. Note that the cloud-base value of the vertical momentum (or mass flux) is used for $(\rho w)^*$ by Arakawa and Schubert.

3. ANALYSES

We have applied the formulation presented in the previous section to four multi-day CRM simulations of deep convective systems. The first one, referred to as DIURNAL, corresponds to the development of diurnal convection over land. The others simulate three distinctively different situations over the western Pacific during the Tropical Ocean Global Atmosphere Coupled Ocean Response Experiment (TOGA-COARE). The first simulation (COARE-Dry) is for a period of suppressed convection following a dry intrusion. The last two correspond to active periods of convection during easterly (COARE-Easterly) and westerly (COARE-Westerly) wind regimes. All the simulations are two-dimensional. The domain horizontal size is $L_x = 512$ km except for COARE-Dry, with $L_x = 100$ km, and it extends vertically above 20 km. The horizontal resolution Δ_x is 2 km, except for COARE-Dry, with $\Delta_x = 1$ km, and the vertical resolution is stretched, ranging from 70 m in the lowest levels to 700 m above 6 km height. The treatments of boundaries are similar among the simulations, all of them using cycling lateral-boundary conditions, together with time-varying prescribed large-scale advectations of heat and moisture derived from observations by following the method proposed in Grabowski *et al.* (1996). For the simulation DIURNAL, surface heat fluxes varying with a diurnal cycle were prescribed. TOGA-COARE observations are based on Ciesielski *et al.* (1997). The simulation DIURNAL is performed with the Meso-NH model (Lafore *et al.* (1998); see also <http://www.aero.obs-mip.fr/mesonh/>), whereas the three other cases use the model developed by Redelsperger and Sommeria (1986)—the RS model in the following. More specific information is provided later for each simulation.

In what follows, the computation of CAPE by Eq. (2) is based on the domain-mean thermodynamic profile of the system with $z_1 = 35$ m, corresponding to the lowest vertical level of the model[†]. No constraint is posed on the sign of buoyancy in this integral. PEC is computed at every grid column as defined by Eq. (5), and its average over the model domain is presented. Data outputs used are instantaneous values for every 12 min for the DIURNAL case, and 5 min for the three COARE cases. Further technical details are presented in the appendix.

(a) *Diurnal convection over land*

This first experiment (DIURNAL) simulates the development of deep convection over land. This run was performed under the European Cloud Project (EUROCS; see <http://www.cnrm.meteo.fr/gcss/EUROCS/main.htm>). The model set-up and the simulation used here are presented in Guichard *et al.* (2004)[‡] and Chaboureau *et al.* (2004), respectively.

This case is particularly interesting, because the diurnal variations of surface heat fluxes (long-dashed curve in Fig. 1(a)) largely control the evolution of CAPE (cf. McBride and Frank 1999; Yano *et al.* 2001; Zhang 2002, 2003; Donner and Phillips 2003). However, in spite of a substantial build-up of CAPE (Fig. 1(b)) by noon, the convective precipitation does not fully develop until afternoon–evening time, a few hours later, as indicated by the total precipitation (solid curve in Fig. 1(a)). It implies that the system is *not* in equilibrium in the sense that the surface forcing is *not* immediately followed by convective precipitation, but the latter response lags behind forcing by

[†] The domain mean is used for CAPE computations because this corresponds to a single-column profile in global models, and also roughly to sounding data. The domain mean of CAPE computed for each CRM column does not provide any noticeable difference.

[‡] See also http://www.cnrm.meteo.fr/gcss/EUROCS/deepdiurmland/idea_index.html

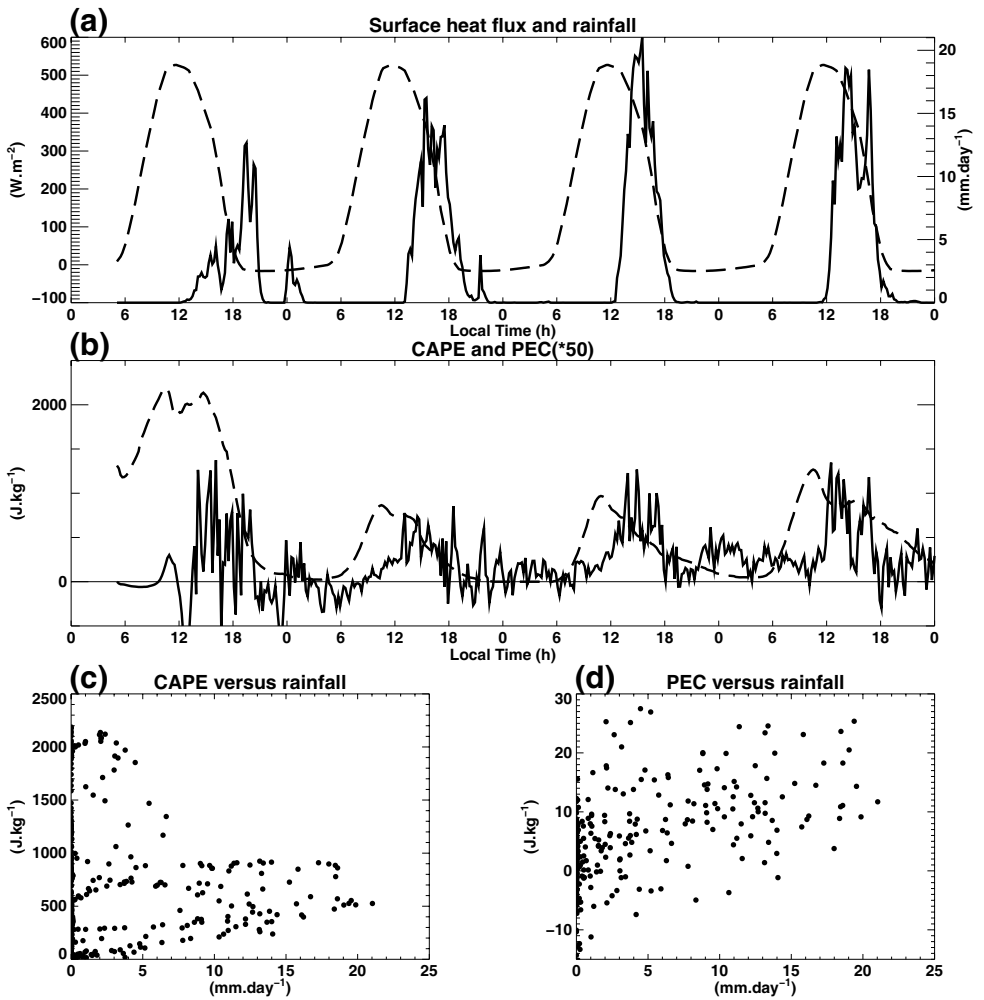


Figure 1. Analysis of the DIURNAL case. Time series of (a) the precipitation rate (solid; $\text{mm}\cdot\text{d}^{-1}$), the surface total heat fluxes (long-dash; $\text{W}\cdot\text{m}^{-2}$), (b) CAPE (long-dash; $\text{J}\cdot\text{kg}^{-1}$), and PEC (solid; $\text{J}\cdot\text{kg}^{-1}$, multiplied by 50). Scatter plots of (c) the precipitation rate and CAPE, (d) the precipitation rate and PEC.

several hours. The mechanisms for such delay as well as those for triggering of late convective events have been the main focuses of this EUROCS study. Here, we argue that CAPE is not a good measure of a degree of convective instability of the system, whereas PEC provides a better quantification, as plotted as the solid curve in Fig. 1 (b), which more closely follows the precipitation time series in Fig. 1(a).

In order to better quantify the degree of correlation of PEC with precipitation, and to compare it with that of CAPE, we show scatter plots of precipitation rate and CAPE, as well as precipitation and PEC in Figs. 1(c) and (d), respectively. Virtually no correlation is found between the precipitation and CAPE (Fig. 1(c)), whereas PEC tends to increase with increasing precipitation (Fig. 1(d)). The correlations of precipitation with CAPE and PEC are 0.11 and 0.44, respectively.

It appears that PEC is much smaller (multiplied by 50 in plot) than CAPE, a result which is consistent with the observational analysis, showing that the buoyancy

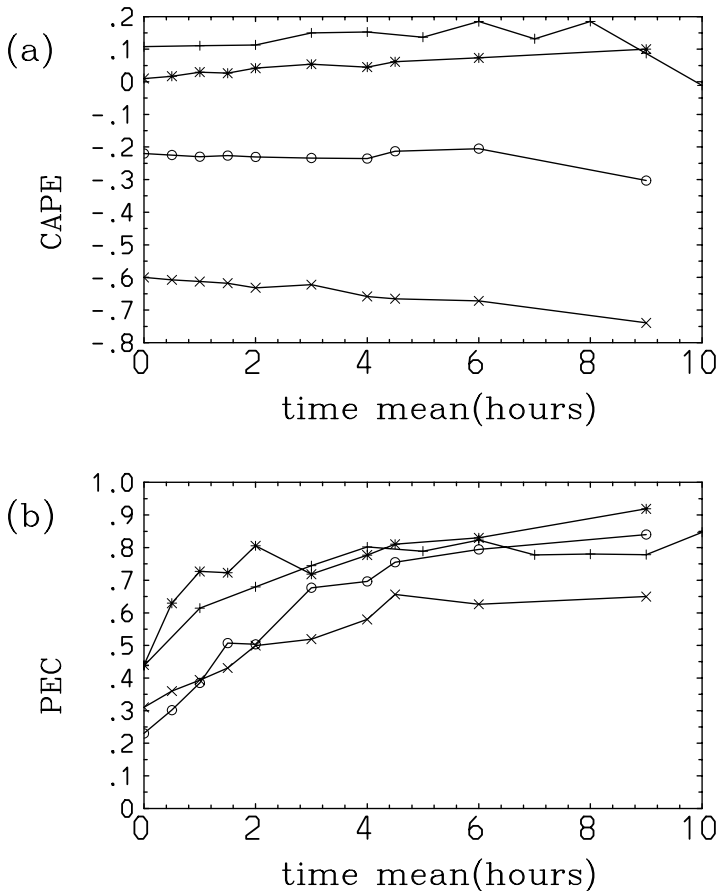


Figure 2. Correlations (a) between the precipitation rate and CAPE, and (b) between the precipitation rate and PEC, as functions of the averaging length in time. The DIURNAL case (as in Fig. 1) is shown by the curve marked by +. The other three curves are for the three experiments: the COARE-Dry (*), the COARE-Easterly (o), and the COARE-Westerly (x) cases. The zero time mean corresponds to the original data, which are given in the interval of 12 min for the DIURNAL case and 5 min for the three COARE cases.

(i.e. virtual-temperature anomaly) within updraught and downdraught cores is much smaller than an undiluted parcel estimate (e.g. Jorgensen and LeMone 1989, their Fig. 13). This indicates that the obtained PEC value is physically sensible, albeit using an arbitrary normalization factor (6).

Although the correlation of precipitation with PEC is clearly higher than the one with CAPE, the former is still quite low. Such a low correlation can be attributed to various reasons. Most importantly, convective precipitation does not necessarily exactly coincide with the convective updraughts generated by PEC, so the instantaneous correlation as taken here is also not necessarily very high. A better correlation is obtained by applying time means to the time series, as shown by a curve with + signs in Fig. 2(b). On the other hand, the correlation between precipitation and CAPE does not improve by applying the time mean (Fig. 2(a)). Precipitation also tends to lag behind PEC, and the maximum lag-correlation 0.58 is obtained with the 40 min lag.

Another obvious factor is that precipitation is not directly generated by PEC, but is generated as a consequence of convective vertical motions, which are generated

TABLE 1. CORRELATIONS OF THE VERTICAL KINETIC ENERGY K_v AND THE PRECIPITATION RATE P WITH VARIOUS MEASURES OF CONVECTIVE INSTABILITY (1ST COLUMN)

	Case	K_v	P
P	DIURNAL	0.57	–
	COARE-Dry	0.76	–
	COARE-Easterly	0.80	–
	COARE-Westerly	0.51	–
CAPE	DIURNAL	0.35	0.11
	COARE-Dry	0.10	0.01
	COARE-Easterly	0.03	–0.22
	COARE-Westerly	0.07	–0.60
$(\rho w)^*$ PEC	DIURNAL	0.57	0.39
	COARE-Dry	0.78	0.56
	COARE-Easterly	0.69	0.47
	COARE-Westerly	0.72	0.42
PEC	DIURNAL	0.49	0.44
	COARE-Dry	0.56	0.43
	COARE-Easterly	0.38	0.23
	COARE-Westerly	0.54	0.31
$(\rho w)^*$	DIURNAL	0.96	0.68
	COARE-Dry	0.92	0.70
	COARE-Easterly	0.94	0.84
	COARE-Westerly	0.96	0.58

by PEC. Thus, the physical relation between precipitation and PEC is rather indirect. In order to investigate this aspect, we have computed the instantaneous correlations between the various related convective variables in Table 1. Even the correlation between the vertical kinetic energy K_v (defined as an average of $w^2/2$ over the two-dimensional domain) and precipitation P is not perfect, reflecting the fact that not all the precipitation of the system is of convective origin, and that convective motions do not systematically generate surface rainfall. Also note that the generation rate for K_v is given by $(\rho w)^*$ PEC, not only by PEC. The former provides a higher correlation with K_v than PEC, but the perfect correlation is attained even for the former only if K_v dissipates with a constant time-scale. The given actual correlation measures a degree that this hypothesis is satisfied. On the other hand, the measure of the vertical motion $(\rho w)^*$ (or horizontal convergence) almost perfectly correlates with K_v , because the vertical motions are dominated by a single vertical structure of the first-baroclinic-type throughout the experiment.

(b) *Dry-intrusion event*

The second experiment (COARE-Dry) simulates a recovering period of the convective atmosphere aftermath of a dry-intrusion event on 14 November 1992 during TOGA-COARE (Redelsperger *et al.* 2002) with use of the RS model.

The intrusion of deep dry air into the modelling domain virtually eliminates moist-convective instabilities of the system, as measured by both CAPE and PEC, as seen in Fig. 3(a). Recovery of the thermodynamic state of the system, as measured by CAPE, is gradual, and stays more or less stationary after two days (cf. Parsons *et al.* 2000, especially their Fig. 14). This gradual recovery of CAPE is contrasted with intermittent rainfall events seen in precipitation time series initiated after one day. In the scatter plot (Fig. 3(b)), we also see virtually no correlation (estimated as 0.01) between precipitation

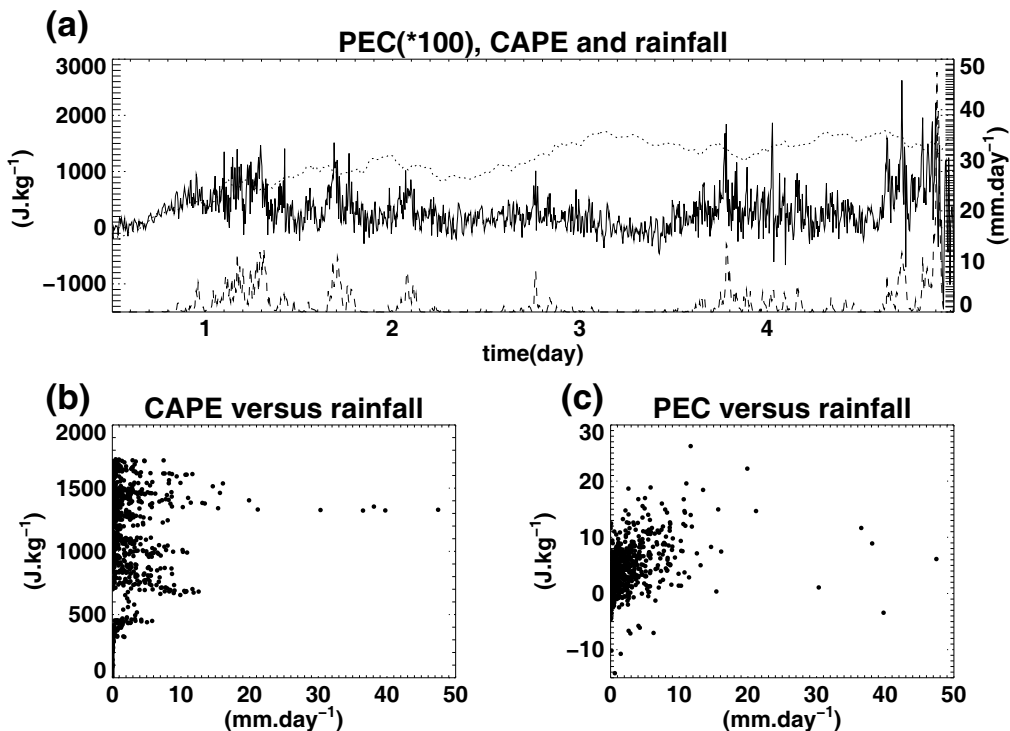


Figure 3. Analysis of the TOGA-COARE dry-intrusion (COARE-Dry) case. (a) Time series of the precipitation rate (long-dash; $\text{mm}\cdot\text{d}^{-1}$), CAPE (short-dash; $\text{J}\cdot\text{kg}^{-1}$), and PEC (solid; $\text{J}\cdot\text{kg}^{-1}$, multiplied by 100). Scatter plots of (b) the precipitation rate and CAPE; (c) the precipitation rate and PEC. The first half day of the experiment is not considered.

rate and CAPE. Here, again, it implies that CAPE is not a good measure of the actual degree of convective instability of the system.

On the other hand, the time series of PEC (Fig. 3(a)) tends to show a tendency to follow the same fluctuations as precipitation. The scatter plot between precipitation and PEC (Fig. 3(c)) also supports the view that these two variables are better correlated (with the estimated correlation 0.43)[†]. This correlation exceeds 0.8 for the 2-hour average time series (Fig. 2(b): the curve marked by *), whereas again, the correlation between precipitation and CAPE remains virtually unchanged by this averaging (Fig. 2(a)). Again, the precipitation also tends to lag behind PEC, and the maximum lag-correlation 0.42 is obtained with the 15 min lag.

(c) Two convective events during TOGA-COARE

The last two experiments analysed here simulate two distinctive convective periods observed during TOGA-COARE with the RS model. The first (COARE-Easterly) concerns the period of 10–17 December 1992 characterized by a weak easterly-wind shear (see Guichard *et al.* (2000) for details) and the second (COARE-Westerly) the period

[†] Note that five points in Fig. 3(c), that are exceptionally associated with high precipitation and low PEC, correspond to a 25 min period towards the end of the 5th day when a short pulsed precipitation event that reaches to $50\text{ mm}\cdot\text{d}^{-1}$ has occurred as seen in Fig. 3(a). These five points are obviously ‘outliers’ that do not contribute to the whole statistics.

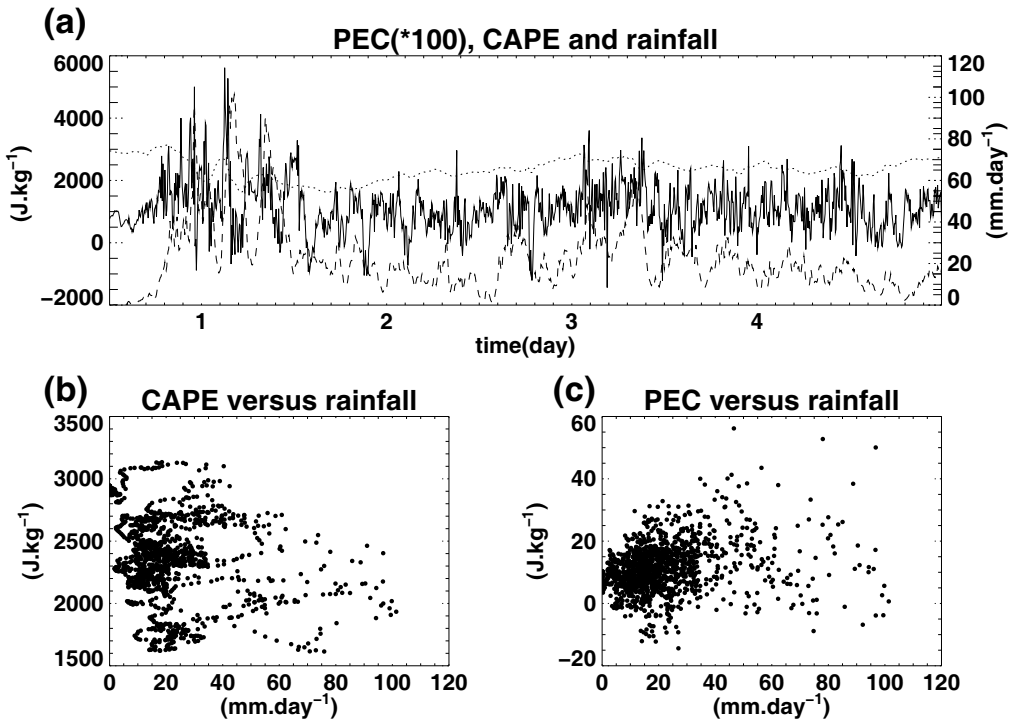


Figure 4. The same as Fig. 3, but for the TOGA-COARE convective easterly-wind regime (COARE-Easterly).

20–26 December 1992, corresponding to a westerly-wind burst event (see Gregory and Guichard (2002) for details, corresponding to the case presented in section 3(b) therein).

The results are shown in Figs. 4 and 5 for these two cases in the same format as in Fig. 3. In both cases, CAPE maintains its high value throughout the period without any mark that it is consumed by convection. The scatter plots (Figs. 4(b) and 5(b)) show that a weak modulation of CAPE is negatively correlated with precipitation in both cases. Thus, CAPE again fails to work as a predictor of convective precipitation. On the other hand, PEC tends to follow the variability of precipitation better as shown both in time series (Figs. 4(a) and 5(a)) and in the scatter plots (Figs. 4(c) and 5(c)). Nevertheless, the obtained correlations (0.23 and 0.31) are lower than the dry-intrusion case, because there are substantial mismatches between the pulsated individual precipitation events and those for PEC, which characterizes these two time series. However, again, this deterioration of statistics is much compensated by the time averaging (Fig. 2(b)). Also the correlation increases as the precipitation lags behind PEC, and reaches the maximum 0.38 and 0.47, respectively, with the lag 55 min and 110 min for the easterly and westerly cases.

4. DISCUSSIONS

From simple physical considerations, we have suggested that CAPE is better interpreted as a measure of an ability of the atmosphere to generate kinetic energy due to moist-convective instabilities. It is indeed such an estimate under a vertical motion with a unit vertical momentum, and by using the buoyancy for a hypothetically lifted air parcel. Along this line of considerations, the concept of CAPE can be naturally

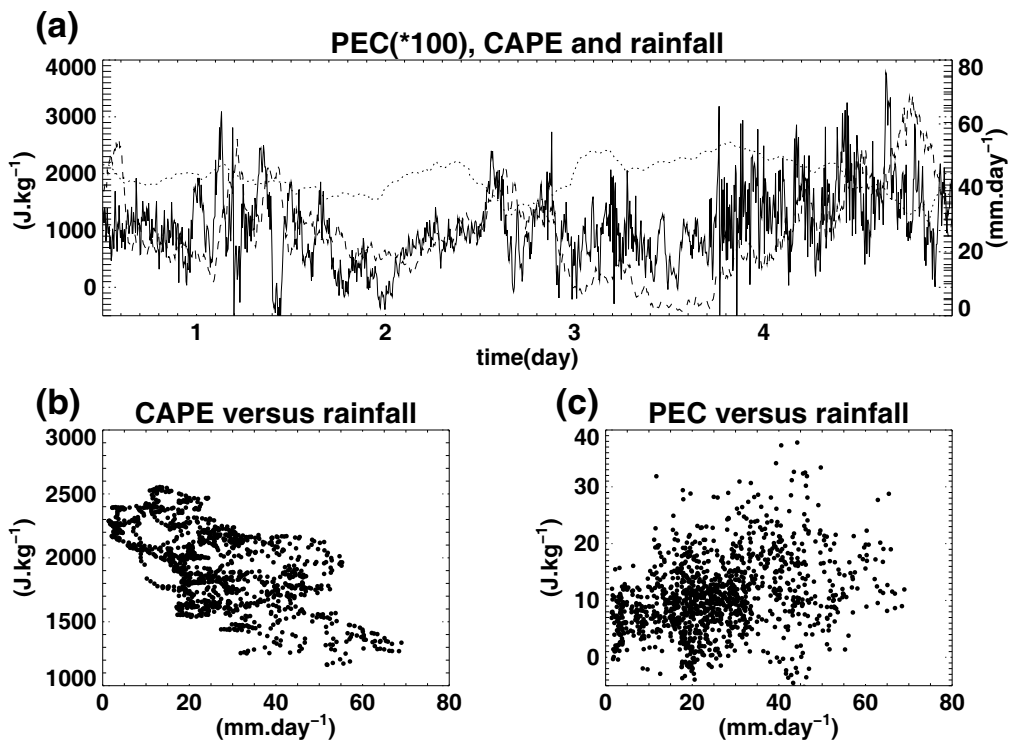


Figure 5. The same as Fig. 3, but for the TOGA-COARE convective westerly-wind regime (COARE-Westerly).

generalized by considering various alternate choices for buoyancy and a *measure* of vertical momentum (*or* normalized vertical momentum). We propose to call this generalization the potential-energy convertibility (PEC). For example, the cloud work function introduced by Arakawa and Schubert (1974) was based on vertical profiles from entraining plumes normalized by a cloud-base vertical momentum (mass flux). In the present work, the buoyancy and normalized vertical momentum are computed as defined locally in CRM at each model grid point, and the model-domain mean is analysed.

A good measure for moist-convective instabilities is something that is missing in the current convective parametrization schemes, as manifested by their general failure to reproduce a time-lag for convective variability by following diurnal forcing (cf. Guichard *et al.* 2004), as discussed in section 3(a). The quasi-equilibrium framework (cf. Randall *et al.* 1997; Yano *et al.* 2000), followed by these schemes in one way or another, combined with standard measures such as CAPE, leads to a prediction of convective variability much in phase with the surface diurnal forcing.

In the present paper, we have shown that PEC as directly estimated from CRM experiments provides a better measure of moist-convective instabilities than the standard CAPE, as manifested by its better correlation with precipitation in time series. Thus, our result suggests that PEC may provide a guidance for defining a measure for moist-convective instabilities in the parametrizations. For this goal, a methodology is to be developed in order to estimate PEC from the grid-box values of global models, although the original PEC has been computed in the convective scales.

Obviously, the undiluted parcel used in the computations of the standard CAPE, regardless of using pseudo-adiabatic or reversible processes (cf. Emanuel 1994; Roff and Yano 2002), are oversimplifications of actual convective updraughts. In fact, many of the current convection schemes (e.g. Fritsch and Chappell 1980; Tiedtke 1989; Gregory and Rowntree 1990; Kain and Fritsch 1990; Zhang and McFarlane 1995; Bechtold *et al.* 2001) use entraining parcel models in order to compute a mean thermodynamics profile for convective updraughts, although assumed entrainment rates are defined in a rather empirical manner[†]. Thus, a possible application of PEC is to use it as a possible methodology for determining these entrainment rates from CRM data objectively.

Here, PEC is estimated by an almost similar manner as in Eq. (2), but replacing the standard parcel buoyancy b by a new one evaluated by including these lateral mixing processes, b^* , i.e.

$$\int_{z_1}^{z_2} b^* dz. \quad (7)$$

Note that Eq. (7) is equivalent to Eq. (5), if this *effective* buoyancy b^* is defined by

$$b^* \equiv \frac{\rho w}{(\rho w)^*} b. \quad (8)$$

Thus, the entrainment rate may be tuned in such way that it produces the *effective* buoyancy b^* consistent with that for PEC, as defined by Eq. (8), leading to a better performance of these parametrizations based on entraining-plume buoyancy.

An alternative approach is to use the mass flux within a convective parametrization as a measure of the vertical momentum in the definition of PEC (Eq. (5)). Finally, it may be important to emphasize that the normalization factor $(\rho w)^*$ in the definition of PEC (Eq. (5)) remains arbitrary. The present definition for $(\rho w)^*$ (Eq. (6)) provides an estimate of a typical buoyancy associated with strong vertical motions (cf. Jorgensen and LeMone 1989, Fig. 13). Nevertheless, a possibility for a renormalization of PEC-based buoyancy (Eq. (8)) could be an important freedom in implementing the present methodology into convective parametrizations.

ACKNOWLEDGEMENTS

The present work has been inspired by Rémi Tailleux, although he chose not to agree with our interpretation on CAPE. It has continuously evolved through discussions with Jean-Luc Redelsperger and Jean-Philippe Lafore under the EUROCS project. Jean-Luc Redelsperger has also kindly provided his dry-intrusion experiment. Comments from Peter Bechtold as well as those from two anonymous reviewers have been helpful for preparing the final manuscript.

APPENDIX

Definitions of variables

Some technical details on the definitions of variables, that are not interesting for general readers, but crucial for reproducing our analyses, are presented here.

[†] However, only a limited number of convective parametrizations in published literatures (Fritsch and Chappell 1980; Gregory *et al.* 2000; Jakob and Siebesma 2003; Kain 2004) explicitly use an entraining parcel for the CAPE computations. Among the others, Gregory and Rowntree (1990) use an entraining parcel for testing the existence of convection, but no CAPE is computed for a closure.

(a) *Density*

The density ρ that should be used in Eq. (5) is the one as used in the mass continuity of the system. A version of Durran’s anelastic system adopted in Meso-NH assumes the mass continuity as given by Eq. (2) of Durran (1989) but neglecting its right-hand side, as suggested by the original author. Thus, it is given by

$$\nabla \cdot \rho_r \theta_{vr} \mathbf{v} = 0, \quad (\text{A.1})$$

where ρ_r is the reference density for the moist air, θ_{vr} the reference profile for the virtual potential temperature, and \mathbf{v} the velocity. It transpires that in this system, $\rho_r \theta_{vr}$ plays the role of density for the mass continuity. For this reason, we set $\rho = \rho_r \theta_{vr} / \theta_0$ with $\theta_0 = 300$ K in analysing the results by the Meso-NH simulation (DIURNAL).

On the other hand, the RS model (CRM used in the other three experiments: Redelsperger and Sommeria (1986)) is based on the anelastic formulation by Lipps and Hemler (1982). In this case, the mass continuity simply uses the reference density so that we set $\rho = \rho_r$.

(b) *Buoyancy*

In defining CAPE, the lifted-parcel buoyancy is defined by

$$b = g \frac{T_{vp} - T_v}{T_v}, \quad (\text{A.2})$$

where g is acceleration of gravity, T_{vp} the lifted-parcel virtual potential temperature following the pseudoadiabatic process (i.e. all the condensed water precipitates out from the parcel), T_v is the virtual temperature of the environment, or as given by the horizontal mean of the model. The surface state of the lifting parcel is also defined by the model domain mean. Definition of the virtual temperature follows that of Emanuel (1994).

On the other hand, in computing PEC, we use the buoyancy as defined in the vertical-momentum equation in the model anelastic systems, i.e.

$$b = g \frac{\theta_v - \theta_{vr}}{\theta_{vr}}, \quad (\text{A.3})$$

where θ_v is the virtual potential temperature as defined at every grid point of the model, whereas θ_{vr} is the same but for the reference profile.

The former is defined by

$$\theta_v = \theta \frac{\{1 + r_v(R_v/R_d)\}}{1 + r_t} \quad (\text{A.4})$$

and

$$\theta_v = \theta \{1 + q_v(R_v/R_d) - q_t\} \quad (\text{A.5})$$

in Meso-NH and the RS model (Redelsperger and Sommeria 1986), respectively. Here, R_v and R_d are the gas constants for water vapour and dry air, respectively; r_v and r_t are the mixing ratios for the water vapour and the total water, respectively, and $q_v = r_v/(1 + r_v)$ and $q_t = r_t/(1 + r_t)$ are the specific humidity and specific content of total water, respectively. Note that the approximations involved in the second definition are consistent with the original model formulation.

The reference profiles are defined by the initial profiles in Meso-NH, and by the domain means at every time step in RS model.

(c) Troposphere height

The troposphere height is defined as $H = 12$ km for the DIURNAL case, $H = 7$ km for the COARE-Dry case, and $H = 15$ km for the two TOGA-COARE convective cases (COARE-Easterly, COARE-Westerly).

REFERENCES

- Arakawa, A. and Schubert, W. H. 1974 Interaction of a cumulus cloud ensemble with the large-scale environment, Part I. *J. Atmos. Sci.*, **31**, 674–701
- Bechtold, P., Bazile, E., Guichard, F., Mascart, P. and Richard, E. 2001 A mass-flux convection scheme for regional and global models. *Q. J. R. Meteorol. Soc.*, **127**, 869–886
- Brown, R. G. and Zhang, C. 1997 Variability of midtropospheric moisture and its effect on cloud-top height distribution during TOGA COARE. *J. Atmos. Sci.*, **54**, 2760–2774
- Chaboureaud, J.-P., Guichard, F., Redelsperger, J.-L. and Lafore, J.-P. 2004 Role of stability and moisture on the diurnal cycle of convection over land. *Q. J. R. Meteorol. Soc.*, **130**, 3105–3117
- Chandrasekhar, S. 1961 *Hydrodynamic and hydromagnetic instability*. Clarendon, Oxford, UK
- Ciesielski, P. E., Hartten, L. M. and Johnson, R. 1997 Impacts of merging profiler and rawinsonde winds on TOGA COARE analyses. *J. Atmos. Oceanic Technol.*, **14**, 1264–1279
- Donner, L. J. and Phillips, V. T. 2003 Boundary layer control on convective available potential energy: Implications for cumulus parameterization. *J. Geophys. Res.*, **108**(D22), doi: 10.1029/2003JD003773
- Durran, D. R. 1989 Improving the anelastic approximation. *J. Atmos. Sci.*, **46**, 1453–1461
- Emanuel, K. A. 1994 *Atmospheric convection*. Oxford University Press
- Fritsch, J. M. and Chappell, C. F. 1980 Numerical prediction of convectively driven mesoscale pressure systems. Part I: Convective parameterization. *J. Atmos. Sci.*, **37**, 1722–1733
- Goldstein, H., Poole, C. and Saffo, J. 2002 *Classical mechanics*, 3rd edition. Addison Wesley, San Francisco, USA
- Grabowski, W. W., Wu, X. and Moncrieff, M. W. 1996 Cloud-resolving modeling of tropical cloud systems during Phase III of GATE. Part I: Two-dimensional experiments. *J. Atmos. Sci.*, **53**, 3684–3709
- Gregory, D. and Guichard, F. 2002 Aspects of the parameterization of organized convection: Contrasting cloud-resolving model and single-column realizations. *Q. J. R. Meteorol. Soc.*, **128**, 625–646
- Gregory, D. and Rowntree, P. R. 1990 A mass flux convection scheme with representation of cloud ensemble characteristics and stability-dependent closure. *Mon. Weather Rev.*, **118**, 1483–1506
- Gregory, D., Morcrette, J.-J., Jakob, C., Beljaars, A. C. M. and Stockdale, T. 2000 Revision of convection, radiation and cloud schemes in the ECMWF Integrated Forecasting System. *Q. J. R. Meteorol. Soc.*, **126**, 1685–1710
- Guichard, F., Redelsperger, J.-L. and Lafore, J.-P. 2000 Cloud-resolving simulation of convective activity during TOGA-COARE: Sensitivity to external sources of uncertainties. *Q. J. R. Meteorol. Soc.*, **126**, 3067–3095
- Guichard, F., Petch, J. C., Redelsperger, J.-L., Bechtold, P., Chaboureaud, J.-P., Cheinet, S., Grabowski, W., Grenier, H., Jones, C. G., Koehler, M., Piriou, J.-M., Tailleux, R. and Tomasini, M. 2004 Modelling the diurnal cycle of deep precipitating convection over land with cloud-resolving models and single-column models. *Q. J. R. Meteorol. Soc.*, **130**, 3139–3172
- Holton, J. R. 1992 *An Introduction to dynamic meteorology* (International Geophysical Series, **48**), 3rd edition. Academic Press, San Diego, USA
- Jakob, C. and Siebesma, A. P. 2003 A new subcloud model for mass-flux convection schemes: Influence on triggering, updraft properties, and model climate. *Mon. Weather Rev.*, **131**, 2765–2778
- Jorgensen, D. P. and LeMone, M. A. 1989 Vertical velocity characteristics of oceanic convection. *J. Atmos. Sci.*, **46**, 621–640

- Kain, J. S. 2004 The Kain–Fritsch convective parameterization: An update. *J. Appl. Meteorol.*, **43**, 170–181
- Kain, J. S. and Fritsch, J. M. 1990 A one-dimensional entraining/detraining plume model and its application in convective parameterization. *J. Atmos. Sci.*, **47**, 2784–2802
- Lafore, J. P., Stein, J., Asencio, N., Bougeault, P., Ducrocq, V., Duron, J., Fischer, C., Hérelil, P., Mascart, P., Masson, V., Pinty, J. P., Redelsperger, J. L., Richard, E. and de Arellano, V.-G. J. 1998 The Meso-NH atmosphere simulation system. Part I: Adiabatic formulation and control simulations. *Ann. Geophys.*, **16**, 90–109
- Lipps, F. B. and Hemler, R. S. 1982 A scale analysis of deep moist convection and some related numerical calculations. *J. Atmos. Sci.*, **39**, 2192–2210
- McBride, J. L. and Frank, W. M. 1999 Relationships between stability and monsoon convection. *J. Atmos. Sci.*, **56**, 24–36
- Mapes, B. E. 1997 ‘Equilibrium vs. activation controls on large-scale variations of tropical deep convection’. Pp. 321–358 in *the Physics and parameterization of moist atmospheric convection*. Ed. R. K. Smith. NATO ASI, Kloster Seon, Kluwer Academic Publishers, Dordrecht, The Netherlands
- Moncrieff, M. W. and Miller, M. J. 1976 The dynamics and simulation of tropical cumulonimbus and squall lines. *Q. J. R. Meteorol. Soc.*, **102**, 373–394
- Parsons, D. B., Yoneyama, K. and Redelsperger, J.-L. 2000 The evolution of the tropical western Pacific atmosphere–ocean system following the arrival of a dry intrusion. *Q. J. R. Meteorol. Soc.*, **126**, 517–548
- Randall, D. A. and Wang, Y. 1992 The moist available energy of a conditional unstable atmosphere. *J. Atmos. Sci.*, **49**, 240–255
- Randall, D., Pan, D.-M., Ding, P. and Cripe, D. G. 1997 ‘Quasi-equilibrium’. Pp. 359–386 in *the Physics and parameterization of moist atmospheric convection*. Ed. R. K. Smith. NATO ASI, Kloster Seon, Kluwer Academic Publishers, Dordrecht, The Netherlands
- Redelsperger, J.-L. and Sommeria, G. 1986 Three-dimensional simulation of a convective storm: Sensitivity studies on subgrid parameterization and spatial resolution. *J. Atmos. Sci.*, **43**, 2619–2635
- Redelsperger, J.-L., Parsons, D. B. and Guichard, F. 2002 Recovery processes and factors limiting cloud-top height following the arrival of a dry intrusion observed during TOGA COARE. *J. Atmos. Sci.*, **59**, 2438–2457
- Roff, G. L. and Yano, J.-I. 2002 Convective variability in the CAPE phase space. *Q. J. R. Meteorol. Soc.*, **128**, 2317–2333
- Rogers, R. R. and Yau, M. K. 1989 *A short course in cloud physics*, 3rd edition. Pergamon, Oxford
- Sherwood, S. C. 1999 Convective precursors and predictability in the tropical western Pacific. *Mon. Weather Rev.*, **127**, 2977–2991
- ter Haar, D. and Wergeland, H. 1966 *Elements of thermodynamics*. Addison-Wesley Pub. Co., Reading, Mass., USA
- Tiedtke, M. 1989 A comprehensive mass flux scheme of cumulus parameterization in large-scale models. *Mon. Weather Rev.*, **117**, 1779–1800
- Xu, K.-M., Arakawa, A. and Krueger, S. K. 1992 The macroscopic behavior of cumulus ensembles simulated by a cumulus ensemble model. *J. Atmos. Sci.*, **49**, 2402–2420
- Yano, J.-I. 1999 Scale-separation and quasi-equilibrium principles in Arakawa and Schubert’s cumulus parameterization. *J. Atmos. Sci.*, **56**, 3821–3823
- Yano, J.-I., Grabowski, W. W., Roff, G. L. and Mapes, B. E. 2000 Asymptotic approaches to convective quasi-equilibrium. *Q. J. R. Meteorol. Soc.*, **126**, 1861–1887
- Yano, J.-I., Fraedrich, K. and Blender, R. 2001 Tropical convective variability as $1/f$ noise. *J. Clim.*, **14**, 3608–3616
- Zhang, G. J. 2002 Convective quasi-equilibrium in midlatitude continental environment and its effect on convective parameterization. *J. Geophys. Res.*, **107**(D14), 4220, doi: 10.1029/2001JD001005
- 2003 Convective quasi-equilibrium in the tropical western Pacific: Comparison with midlatitude continental environment. *J. Geophys. Res.*, **108**, D19, 4592, doi: 10.1029/2003JD003520
- Zhang, G. J. and McFarlane, N. A. 1995 Sensitivity of climate simulations to the parameterization of cumulus convection in the Canadian Climate Centre general circulation model. *Atmos. Ocean*, **33**, 407–446